

# Wigner description of massless Dirac plasmas

J. L. Figueiredo,<sup>1,2,\*</sup> J. P. Bizarro,<sup>1,2</sup> and H. Terças<sup>1,2</sup>

<sup>1</sup>*Instituto de Plasmas e Fusão Nuclear, Lisboa, Portugal*

<sup>2</sup>*Instituto Superior Técnico, Lisboa, Portugal*

We derive a quantum kinetic model describing the dynamics of graphene electrons in phase space based on the Wigner-Moyal procedure. In order to take into account the quantum nature of the carriers, we start from the low-energy Schrödinger equation describing the mean-field wavefunction for both the conduction and valence electrons. The equation of motion for the Wigner matrix is established, with the Coulomb interaction being introduced self-consistently (in the Hartree approximation). The long wavelength limit for the plasmon dispersion relation is obtained, for both ungated and gated situations. As an application, we derive the corresponding hydrodynamical equations and add discuss the correct value of the effective hydrodynamic mass of the carriers from first principles, an issue that is crucial in the establishment of the correct hydrodynamics of Dirac electrons, thus paving the stage towards a more comprehensive description of graphene plasmonics.

## I. INTRODUCTION

In the recent years, graphene has been extensively studied due to its spectacular optical, electronic and mechanical properties [1]. In addition to its two-dimensional (2D) nature, the elementary electronic excitations are described by a Dirac-like dispersion in the low-energy limit [2, 3]. The relativistic nature of graphene electrons, resulting from the cone-like dispersion relation near the Dirac points, makes it useful for transparent electronic devices, ultra-sensitive photodetectors and other high-performance optoelectronic structures [4–6]. Furthermore, graphene possesses extremely high quantum efficiency for light-matter interactions [7]. Moreover, the collective oscillations of the electron and hole densities lead to the formation of plasmons (or plasma waves) [8]. In fact, plasmonics of 2D materials, such as graphene and transition metal dichalcogenides (TMDCs) and hexagonal boron nitride (hBN) [9, 10], is nowadays a very prominent field of research [11]. Graphene-based plasmonics finds a variety of applications, as the versatility of graphene enables the manufacture of optical devices working in different frequency ranges, namely in the terahertz (THz) and the infrared domains [12]. While metal plasmonics exhibit large Ohmic losses, which limits their applicability to optical processing devices, doped graphene emerges as an alternative. Its large conductivity, in part due to the zero-mass character of the carriers, encloses a wide range of potential applications, such as high-frequency nanoelectronics, nanomechanics, transparent electrodes, and composite materials [13]. For this reason, the possibility of electric gating has been extensively studied in graphene, allowing for the manipulation of the Fermi level [14]. Recently, gating with a solid electrolyte allowed carrier concentrations as large as  $10^{14} \text{ cm}^{-2}$  to be achieved, which results in a Fermi energy of  $E_F \simeq 1 \text{ eV}$ , such that a modulation of optical transmission in the visible spectrum is

possible [15, 16]. The potentiality of THz emission was also pointed out [17] as a possible application recently, by making use of a graphene field-effect transistor (gFET), and controlling the applied gate voltage and injected current.

From the theoretical point of view, a variety of techniques have been developed to establish the dynamics of Dirac electrons and holes in graphene, ranging from semiclassical hydrodynamical models [18–20] to quantum formalisms that involve collective Green’s functions, such as the time-dependent Hartree-Fock approximation [21, 22], or the time-dependent density functional theory [23]. In one hand, it is often the case that, when going towards a complete quantum description, cumbersome equations crop up, which are of very reduced utility; on the other, the semiclassical approach is based on the Vlasov equation, which is adequate in the case of high temperatures and low electron-hole densities, but may fail to describe other important quantum phenomena [24].

In this work, we establish a kinetic formalism based on Wigner’s formulation of quantum mechanics to study the Dirac electrons and holes in phase space [25]. We start by constructing a Schrödinger equation for the conduction and valence electrons, derived from a microscopic tight-binding model, for the low-energy electrons. After moving to the electron-hole basis, we derive a kinetic equation for the Wigner matrix components, which correctly incorporates the pseudo-spin degrees of freedom. The interaction is introduced self-consistently via the Hartree approximation, which obeys the Poisson equation. With this in hand, we are able to obtain the plasmon dispersion relation, recovering the usual result based on the random-phase approximation (RPA). By performing averages over the phase-space distributions (more precisely, by taking the moments of the Wigner equation), hydrodynamical equations are obtained allowing for a fluid description of the Dirac particles in graphene. As a consequence, we are able to derive microscopically the effective mass of a fluid particle and relate it to the Drude mass, thus contributing to the understanding of an important question in graphene hydrodynamics. We also show that the classical limit corresponds to previous results based

\* jose.luis.figueiredo@tecnico.ulisboa.pt

on the Vlasov equation for the classical distribution function.

## II. GRAPHENE PRELIMINARIES

The electronic dynamics can be captured starting with a general form for the Hamiltonian, written in a second quantized fashion,

$$\hat{H} = \sum_{s,s'} \sum_{\mathbf{R},\mathbf{R}'} \hat{u}_s^\dagger(\mathbf{R}) \langle \hat{u}_s, \mathbf{R} | \hat{H} | \hat{u}_{s'}, \mathbf{R}' \rangle \hat{u}_{s'}(\mathbf{R}'), \quad (1)$$

where  $\mathbf{R}/\mathbf{R}'$  run over the real lattice, and  $s/s'$  over the two sublattices  $A$  and  $B$ . Additionally,  $\hat{u}_s^\dagger(\mathbf{R})$  and  $\hat{u}_s(\mathbf{R})$  denote the creation and annihilation operators, respectively, for each lattice point  $\mathbf{R}$  and sublattice  $s$ . Moreover, the tight-binding approximation can be settled with a proper restriction on the matrix elements  $\langle \hat{u}_s, \mathbf{R} | \hat{H} | \hat{u}_{s'}, \mathbf{R}' \rangle$ . By allowing hopping only between nearest neighbors, we can set all matrix elements to zero except the cases of  $\langle \hat{u}_s, \mathbf{R} | \hat{H} | \hat{u}_{s'}, \mathbf{R} + \boldsymbol{\delta}_i \rangle = -t(1 - \delta_{ss'})$ , where  $t \simeq 2.97$  eV is the hopping integral and  $\boldsymbol{\delta}_i$  are the

nearest-neighbor vectors [3]. In momentum space, the Hamiltonian reduces to

$$\hat{H} = \sum_{\mathbf{q}} \boldsymbol{\varphi}_{\mathbf{q}}^\dagger \begin{pmatrix} 0 & -t\Delta \\ -t\Delta^* & 0 \end{pmatrix} \boldsymbol{\varphi}_{\mathbf{q}}, \quad (2)$$

where  $\mathbf{q} = (q_x, q_y)$  is the wave-vector,  $\boldsymbol{\varphi}_{\mathbf{q}} = (\hat{u}_{A\mathbf{q}}, \hat{u}_{B\mathbf{q}})^T$  and  $\Delta(\mathbf{q}) = \sum_i e^{-i\mathbf{q} \cdot \boldsymbol{\delta}_i}$ . We can diagonalize Eq. (2) by the means of a similarity transformation  $\boldsymbol{\Phi}(\mathbf{q}, t) = S\boldsymbol{\varphi}(\mathbf{q}, t)$ , where  $\boldsymbol{\Phi}^T(\mathbf{q}, t) = (\hat{c}_{\mathbf{q}}, \hat{v}_{\mathbf{q}})$  and  $\hat{c}_{\mathbf{q}}$  and  $\hat{v}_{\mathbf{q}}$  respectively denote conduction and valence electron annihilation operators. Plugging in Eq. (2), we obtain

$$\hat{H} = \sum_{\mathbf{q}} \boldsymbol{\Phi}_{\mathbf{q}}^\dagger \begin{pmatrix} \hbar\omega(\mathbf{q}) & 0 \\ 0 & -\hbar\omega(\mathbf{q}) \end{pmatrix} \boldsymbol{\Phi}_{\mathbf{q}}, \quad (3)$$

where

$$S = \frac{1}{\sqrt{2}} \begin{pmatrix} -e^{-i\theta(\mathbf{q})} & 1 \\ e^{i\theta(\mathbf{q})} & 1 \end{pmatrix}, \quad (4)$$

$e^{i\theta(\mathbf{q})} = \sqrt{\Delta(\mathbf{q})/\Delta^*(\mathbf{q})}$ , and

$$\hbar\omega(\mathbf{q}) = t\sqrt{\cos\left(\sqrt{3}dq_x/2\right)\cos\left(3dq_y/2\right) + 2\cos\left(\sqrt{3}dq_x\right) + 3}, \quad (5)$$

is the single-particle dispersion relation. Above,  $d \simeq 1.5$  Å is the carbon-carbon distance, related to the lattice parameter  $a$  as  $a = \sqrt{3}d$ . We can expand Eq. (3) around the Dirac point  $\mathbf{K} = (4\pi/3\sqrt{3}d, 0)$  and obtain [26]

$$\omega(\mathbf{q}) \simeq v_F|\mathbf{q}|, \quad (6)$$

where  $v_F = 3ta/(2\hbar) \simeq 10^6$  ms<sup>-1</sup> is the Fermi velocity. As such, the low-energy Hamiltonian in Fourier space yields

$$\hat{H} = \sum_{\mathbf{q}} \xi(\mathbf{q}) (\hat{c}_{\mathbf{q}}^\dagger \hat{c}_{\mathbf{q}} - \hat{v}_{\mathbf{q}}^\dagger \hat{v}_{\mathbf{q}}), \quad (7)$$

where  $\xi(\mathbf{q}) = \hbar v_F|\mathbf{q}|$  is the single-particle dispersion relation near the Dirac point.

By inspecting Eq. (7), we still face the problem of treating negative-energy excitations. To circumvent it, we move to the electron-hole basis by defining the (fermionic) hole creation and annihilation operators,  $\hat{h}_{\mathbf{q}}^\dagger = \hat{v}_{-\mathbf{q}}$  and  $\hat{h}_{\mathbf{q}} = \hat{v}_{\mathbf{q}}^\dagger$ , and by setting the vacuum (Fermi sea) as

$$|\Omega_F\rangle = \prod_{\mathbf{q}} \hat{v}_{\mathbf{q}}^\dagger |0\rangle. \quad (8)$$

The latter is related to the Fermi level as  $\hat{H}|\Omega_F\rangle = E_F|\Omega_F\rangle$ , where  $E_F$  is the Fermi energy. In this new basis,

the Hamiltonian in Eq. (7) reads

$$\hat{H} = E_F + \sum_{\mathbf{q}} \xi(\mathbf{q}) (\hat{c}_{\mathbf{q}}^\dagger \hat{c}_{\mathbf{q}} + \hat{h}_{\mathbf{q}}^\dagger \hat{h}_{\mathbf{q}}). \quad (9)$$

We now write the equation of motion for both electrons and holes,  $i\hbar\partial_t\boldsymbol{\psi} = \hat{H}\boldsymbol{\psi}$ , where  $\boldsymbol{\psi}^T(\mathbf{q}, t) = (\hat{c}_{\mathbf{q}}, \hat{h}_{\mathbf{q}})$ . In what follows, we shall drop the constant  $E_F$ , for simplicity. Then, the Hamiltonian  $\hat{H}$  comprises kinetic and potential terms, accounting for the Coulomb interaction, which leads to

$$i\hbar\frac{\partial}{\partial t}\boldsymbol{\psi}^\alpha(\mathbf{q}, t) = \xi(\mathbf{q})\boldsymbol{\psi}^\alpha(\mathbf{q}, t) + \int d\mathbf{q}' V^\alpha(\mathbf{q}', t)\boldsymbol{\psi}^\alpha(\mathbf{q} - \mathbf{q}', t). \quad (10)$$

Here,  $V^\alpha(\mathbf{q}, t) = \mathcal{Q}^\alpha\phi(\mathbf{q}, t)$ ,  $\mathcal{Q}^\alpha$  is the charge of the carriers of band  $\alpha$  and  $\phi(\mathbf{q}, t)$  is the Fourier transform of the electrostatic potential. In real space,  $\phi$  satisfies the Poisson equation

$$\nabla^2\phi = -\frac{1}{\epsilon_0\epsilon_r} \sum_{\beta} \mathcal{Q}^\beta n^\beta, \quad (11)$$

with  $n^\beta(\mathbf{r}, t) = |\psi^\beta(\mathbf{r}, t)|^2$  denoting the electron ( $\beta = 1$ ) and hole ( $\beta = 2$ ) densities. We perform our calculations

within the Hartree (mean-field) approximation, thus neglecting exchange contributions (correlations). This procedure is valid for small values of the coupling parameter  $r_s \sim \alpha_s/\varepsilon_r$  (ratio of the average potential energy to the average kinetic energy), where  $\alpha_s = e^2/(4\pi\varepsilon_0\hbar v_F) \simeq 2.2$  is the graphene structure constant. As a result, the Hartree approximation is reliable as long as  $\varepsilon_r \gtrsim 2.2$ . A formal solution to Eq. (11) can be written as

$$\phi(\mathbf{r}, t) = \frac{1}{4\pi\varepsilon_0\varepsilon_r} \int d\mathbf{r}' \sum_{\beta} \frac{\mathcal{Q}^{\beta} n^{\beta}(\mathbf{r}', t)}{|\mathbf{r} - \mathbf{r}'|}, \quad (12)$$

thus providing a closure relation to the system of Eq. (10). In other words, we have

$$\phi(\mathbf{q}, t) = \mathcal{U}(\mathbf{q}) \sum_{\beta} s^{\beta} n^{\beta}(\mathbf{q}, t), \quad (13)$$

where  $\mathcal{U}(\mathbf{q}) = e/2\varepsilon_0\varepsilon_r|\mathbf{q}|$  is the 2D Fourier transform of the Coulomb potential,  $e = |e|$  is the elementary charge and  $s^{\beta} = 2\beta - 3$  is the sign of the  $\beta$ -charge.

### III. WIGNER FORMALISM

A very handy way to treat the electronic system of (10) is by using the Wigner picture of quantum mechanics [25], which allows for a fully phase-space description, in close analogy with the classical case. In the classical limit, the Wigner function denotes the probability density of finding a particle in a given infinitesimal phase space volume  $d\mathbf{r} d\mathbf{k}$  centred in  $(\mathbf{r}, \mathbf{k})$ . In the quantum case, due to the commutation relation between  $\mathbf{r}$  and  $\mathbf{q}$ , the Heisenberg uncertainty principle prevents particles to localize in a specific phase-space point, and a proper distribution function is not possible to construct [27]. However, we can still construct the Wigner function  $W(\mathbf{r}, \mathbf{k}, t)$  whose properties are similar to those of a classical distribution function. It is a function of both a spatial coordinate  $\mathbf{r}$  and a wave-vector coordinate  $\mathbf{k}$ . Although  $\mathbf{r}$  and  $\mathbf{k}$  are not conjugated to each other, they both give information about the spatial and momentum distributions of the system, which is described by

a wave-function  $\psi(\mathbf{r}, t)$ . The phase-space regions where  $W(\mathbf{r}, \mathbf{k}, t)$  takes negative values are purely quantum, having no classical analogue as it cannot be univocally defined as a particle phase-space density. For that reason, the Wigner function is often referred to as a quasi-distribution function. The mathematical definition of the Wigner function is given by the Weyl transform [28] of the density operator  $\hat{\rho}$ . The expectation values of any operator can be computed by integrating the Weyl transform of the same operator multiplied by  $W(\mathbf{r}, \mathbf{k}, t)$ , very similarly to the classical case [29]. For the present case, it is given by a tensor  $W^{\alpha\gamma}(\mathbf{r}, \mathbf{k}, t)$ , accounting for the pseudo-spin degrees of freedom,

$$W^{\alpha\gamma}(\mathbf{r}, \mathbf{k}, t) = \int \frac{d\mathbf{s}}{(2\pi)^2} e^{i\mathbf{k}\cdot\mathbf{s}} \times \psi^{\alpha}(\mathbf{r} - \mathbf{s}/2, t) \psi^{*\gamma}(\mathbf{r} + \mathbf{s}/2, t). \quad (14)$$

Although the diagonal is real, the off-diagonal elements can have non-zero imaginary parts (despite being complex-conjugated to each other). Those elements represent the density correlations between the two populations. Notwithstanding, in the present mean-field approximation, the off-diagonal elements decouple, and will thus be neglected. The potential in Eq. (13) can be calculated self-consistently from the diagonal components as (no summation)

$$n^{\alpha}(\mathbf{r}, t) = \int d\mathbf{k} W^{\alpha\alpha}(\mathbf{r}, \mathbf{k}, t), \quad (15)$$

while in momentum space Eq. (14) transforms to

$$W^{\alpha\gamma}(\mathbf{q}, \mathbf{k}, t) = \psi^{\alpha}(\mathbf{k} + \mathbf{q}/2, t) \psi^{*\gamma}(\mathbf{k} - \mathbf{q}/2, t). \quad (16)$$

To construct an equation for the Wigner matrix, we start by writing Eq. (10) and its hermitian conjugate for two independent momentum coordinates,  $\mathbf{q}_1$  and  $\mathbf{q}_2$ , and distinct pseudo-spin indices,  $\alpha$  and  $\gamma$ . By multiplying the first by  $\psi^{*\gamma}(\mathbf{q}_2, t)$  and the second by  $\psi^{\alpha}(\mathbf{q}_1, t)$  and subtracting the equations, we obtain

$$i\hbar \frac{\partial}{\partial t} [\psi^{\alpha}(\mathbf{q}_1, t) \psi^{*\gamma}(\mathbf{q}_2, t)] = [\xi(\mathbf{q}_1) - \xi(\mathbf{q}_2)] \psi^{\alpha}(\mathbf{q}_1, t) \psi^{*\gamma}(\mathbf{q}_2, t) + \int d\mathbf{q}' [V^{\alpha}(\mathbf{q}', t) \psi^{\alpha}(\mathbf{q}_1 - \mathbf{q}', t) \psi^{*\gamma}(\mathbf{q}_2, t) - V^{\gamma}(\mathbf{q}', t) \psi^{\alpha}(\mathbf{q}_1, t) \psi^{*\gamma}(\mathbf{q}_2 - \mathbf{q}', t)], \quad (17)$$

where we used  $V^{\alpha}(\mathbf{q}', t)^* = V^{\alpha}(-\mathbf{q}', t)$ . Recalling the identity  $f(\mathbf{k} + \mathbf{q}) = e^{\mathbf{q}\cdot\nabla_{\mathbf{k}}} f(\mathbf{k})$ , and introducing the coordinate transformation  $\mathbf{q}_1 = \mathbf{k} + \mathbf{q}/2$ ,  $\mathbf{q}_2 = \mathbf{k} - \mathbf{q}/2$  into

Eq. (17), it follows, after some straightforward algebra

$$\left[ i\hbar \frac{\partial}{\partial t} - \Delta\xi^{-}(\mathbf{q}, \mathbf{k}) \right] W^{\alpha\gamma}(\mathbf{q}, \mathbf{k}, t) = e \int d\mathbf{q}' \phi(\mathbf{q}', t) \times \Delta W^{\alpha\gamma}(\mathbf{q}, \mathbf{k}, \mathbf{q}', t), \quad (18)$$

where  $\Delta W^{\alpha\gamma}(\mathbf{q}, \mathbf{k}, \mathbf{q}', t) = s^\alpha W^{\alpha\gamma}(\mathbf{q} - \mathbf{q}', \mathbf{k} - \mathbf{q}'/2, t) - s^\gamma W^{\alpha\gamma}(\mathbf{q} - \mathbf{q}', \mathbf{k} + \mathbf{q}'/2, t)$  and  $\Delta\xi^-(\mathbf{q}, \mathbf{k}) = \xi(\mathbf{k} + \mathbf{q}/2) - \xi(\mathbf{k} - \mathbf{q}/2)$ . Equations (18) and (13) define the Wigner-Poisson model for 2D Dirac particles in Fourier space. For the diagonal components  $W^{\alpha\alpha}(\mathbf{r}, \mathbf{k}, t) \doteq W^\alpha$ , the real space version of Eq. (18) reads

$$i\hbar \frac{\partial}{\partial t} W^\alpha + i\hbar \mathcal{K}\{W^\alpha\} = \int d\mathbf{q} e^{i\mathbf{q}\cdot\mathbf{r}} \left( W_-^\alpha - W_+^\alpha \right) \times V^\alpha(\mathbf{q}, t), \quad (19)$$

where  $W_\pm^\alpha \doteq W^\alpha(\mathbf{r}, \mathbf{k} \pm \mathbf{q}/2, t)$  and

$$\mathcal{K}\{W^\alpha\} = v_F \int \frac{d\mathbf{r}'}{(2\pi)^2} \frac{\sin(2\mathbf{k} \cdot \mathbf{r}')}{|\mathbf{r}'|^3} W^\alpha(\mathbf{r} - \mathbf{r}', \mathbf{k}, t), \quad (20)$$

represents the kinetic operator. Its nonlocal nature is profoundly related to the relativistic nature of the Dirac electrons, and strongly differs from the term appearing in semi-classical equations proposed in the literature,  $\mathcal{K}\{W^\alpha\} = \mathbf{v}_\mathbf{k} \cdot \nabla W^\alpha$ , with  $\hbar \mathbf{v}_\mathbf{k} = \partial_\mathbf{k} \xi(\mathbf{k}) = \hbar v_F \mathbf{k}/|\mathbf{k}|$  (see Ref. [30] and references therein). It is convenient to compare it with the conventional parabolic dispersion relation,  $\xi(\mathbf{k}) = \hbar^2 \mathbf{k}^2/(2m)$ , for which the kinetic operator reduces to the usual (local) convective derivative [29]

$$\mathcal{K}\{W^\alpha\} = \frac{\hbar \mathbf{k}}{m} \cdot \nabla W^\alpha. \quad (21)$$

Moreover, in the limit  $\hbar \rightarrow 0$ , we can approximate  $W_\pm^\alpha$  as

$$W_\pm^\alpha \simeq W^\alpha \pm \frac{\hbar \mathbf{q}}{2} \cdot \nabla_\mathbf{p} W^\alpha, \quad (22)$$

with  $\mathbf{p} = \hbar \mathbf{k}$ , which allows us to write the ray-tracing version of Eq. (19) as (no summation)

$$\frac{\partial}{\partial t} W^\alpha + \frac{\mathbf{p}}{m} \cdot \nabla W^\alpha - \nabla V^\alpha \cdot \nabla_\mathbf{p} W^\alpha \simeq 0. \quad (23)$$

This means that, for parabolic particles, the classical limit of the Wigner equation corresponds to the Vlasov equation. However, no classical limit of Eq. (20) exists (i.e. it does not converge as  $\hbar \rightarrow 0$ ), which then confers to Dirac particles a purely quantum nature.

We now consider small perturbations around an equilibrium configuration, keeping the lowest order contributions to the Wigner components. As such, we can write

$$W^{\alpha\gamma}(\mathbf{r}, \mathbf{k}, t) \simeq W_0^\alpha(\mathbf{k}) \delta^{\alpha\gamma} + \tilde{W}^{\alpha\gamma}(\mathbf{r}, \mathbf{k}, t), \quad (24)$$

with  $|\tilde{W}^{\alpha\gamma}| \ll W_0^\alpha$ , which in momentum space reads  $W^{\alpha\gamma}(\mathbf{q}, \mathbf{k}, t) \simeq W_0^\alpha(\mathbf{k}) \delta(\mathbf{q}) \delta^{\alpha\gamma} + \tilde{W}^{\alpha\gamma}(\mathbf{q}, \mathbf{k}, t)$ . Similarly, the density and electrostatic potential will be perturbed as

$$n^\alpha(\mathbf{q}, t) \simeq n_0^\alpha \delta(\mathbf{q}) + \tilde{n}^\alpha(\mathbf{q}, t), \quad (25)$$

$$\phi(\mathbf{q}, t) \simeq \mathcal{U}(\mathbf{q}) \sum_\beta [n_0 \delta(\mathbf{q}) + \tilde{n}^\beta(\mathbf{q}, t)], \quad (26)$$

where  $n_0^\alpha = \int d\mathbf{k} W_0^\alpha(\mathbf{k})$  is the equilibrium density of each band. We can show that the lowest order contributions of Eq. (18) vanish. Moreover, the first order terms provide

$$i\hbar \frac{\partial}{\partial t} \tilde{W}^{\alpha\gamma}(\mathbf{q}, \mathbf{k}, t) = \Delta\xi^-(\mathbf{q}, \mathbf{k}) \tilde{W}^{\alpha\gamma}(\mathbf{q}, \mathbf{k}, t) + \sum_\beta \tilde{n}^\beta(\mathbf{q}, t) \times \mathcal{Q}^\alpha \mathcal{U}(\mathbf{q}) \Delta W_0^\alpha(\mathbf{k}, \mathbf{q}) \delta^{\alpha\gamma}, \quad (27)$$

where  $\Delta W_0^\alpha(\mathbf{k}, \mathbf{q}) = W_0^\alpha(\mathbf{k} - \mathbf{q}/2) - W_0^\alpha(\mathbf{k} + \mathbf{q}/2)$ . Equation (27) is formally equivalent to Kubo's formula for the linear response of a many-body system [31] and reproduces the features contained in RPA [32, 33]. This formalism is specially advantageous to describe the dynamics of electrons that are far from equilibrium, such as the case of plasma instabilities, with the configuration being solely defined by  $W_0$ .

In what follows, we consider the case of negatively doped graphene, with the conduction band filled up to the Fermi level  $E_F > 0$ . In momentum-energy space, this is defined by the cone  $E(\mathbf{k}) = \hbar v_F |\mathbf{k}| \Theta(k_F - |\mathbf{k}|)$ , where  $\Theta(x)$  is the Heaviside step function, and  $k_F = E_F/(\hbar v_F)$  is the Fermi wave-number. The latter is related with the doping density  $n_0$  by

$$k_F = \sqrt{\frac{4\pi n_0}{g_s g_v}}, \quad (28)$$

where  $g_s g_v$  accounts for the spin ( $g_s = 2$ ) and valley ( $g_v = 2$ ) degeneracy. The first results from the degeneracy of the spin populations in each energy band, which we have neglected in our treatment so far, and the latter should be incorporated to consistently include the two minima in the first Brillouin zone (BZ) [34]. Typical experimental values of  $n_0$  between  $10^9 - 5 \times 10^{12} \text{ cm}^{-2}$  are achievable in graphene [35]. In the case  $E_F \gg k_B T$ , the presence of holes is negligible, which allows us to set  $\tilde{W}^{22} = 0$  and solve Eq. (18) for the Wigner component  $\tilde{W}^{11}$  (notice that the off-diagonal terms  $W^{12}$  and  $W^{21}$  are also not relevant in that case; we also simplify the notation by dropping the superscripts,  $W \doteq W^{11}$  and  $n \doteq n_1$ ). After Fourier transforming the time coordinate, we can recast Eq. (27) into a more familiar form,

$$\tilde{W}(\mathbf{q}, \mathbf{k}, \omega) = \tilde{n}(\mathbf{q}, t) \mathcal{U}(\mathbf{q}) \frac{\Delta W_0(\mathbf{k}, \mathbf{q})}{\hbar\omega - \xi(\mathbf{k} + \mathbf{q}/2) + \xi(\mathbf{k} - \mathbf{q}/2)}. \quad (29)$$

Upon integrating both sides in  $\mathbf{k}$ , we obtain the dielectric function

$$\epsilon(\mathbf{q}, \omega) = 1 - \mathcal{U}(\mathbf{q}) \Pi(\mathbf{q}, \omega), \quad (30)$$

where the polarizability function  $\Pi(\mathbf{q}, \omega)$  is defined as

$$\Pi(\mathbf{q}, \omega) = \int d\mathbf{k} \frac{W_0(\mathbf{k}) - W_0(\mathbf{k} + \mathbf{q})}{\hbar\omega + \xi(\mathbf{k}) - \xi(\mathbf{k} + \mathbf{q})}. \quad (31)$$

The plasmon dispersion relation is given by the zeros of  $\epsilon(\mathbf{q}, \omega)$ . We note that, in the absence of streaming,  $\epsilon(\mathbf{q}, \omega)$  and  $\omega(\mathbf{q})$  depend only on  $q \doteq |\mathbf{q}|$ . The formal result of

Eq. (30) is equivalent to the RPA [32]. In the long wavelength limit  $q \rightarrow 0$ , the plasmon frequency can be computed using the noninteracting irreducible polarizability, and Eq. (30) is recovered. We assume the equilibrium configuration to be given by

$$W_0(\mathbf{k}) = n_0 \Theta(k_F - |\mathbf{k}|) / \pi k_F^2, \quad (32)$$

and expanding Eq. (30) around  $q = 0$ , keeping only terms up to  $\mathcal{O}(q^2)$ , the plasmon dispersion relation is obtained

$$\omega^2 = \omega_p^2 \frac{q}{k_F} + \frac{3}{4} v_F^2 q^2, \quad (33)$$

where  $\omega_p$  is the characteristic plasmon frequency

$$\omega_p = \left( \frac{e^2 n_0 v_F}{2 \hbar \varepsilon_0 \varepsilon_r} \right)^{1/2}. \quad (34)$$

For the typical experimental values  $\varepsilon_r = 2.5$  and  $n_0 \in [5 \times 10^{-3}, 1] \times 10^{12} \text{ cm}^{-2}$ ,  $\omega_p$  lies in the THz-region,  $\omega_p \in [2.6, 37.3] \text{ THz}$ . The first term  $\omega \sim \sqrt{q}$  describes the long wavelength signature of plasmons in two-dimensional electron gases (2DEG) [36–39]. The most notable difference, when compared to the characteristic plasmon frequency in the 3-dimensional parabolic case,  $\omega_p^{3D} = \sqrt{e^2 n_0 / (\varepsilon_0 \varepsilon_r m)}$ , is the appearance of  $\hbar$  in leading order, revealing its pure quantum nature. Therefore, no classical counterpart exists for the 2D Dirac plasma, which confirms our previous observation.

The same kinetic approach can be used to describe graphene electrons in a field effect transistor (FET) structure, i.e., placed between two metallic contacts, source and drain, and controlled by a gate. The gate voltage is related to the carrier density by [40]

$$U(\mathbf{r}, t) = e n(\mathbf{r}, t) \left( \frac{1}{C_g} + \frac{1}{C_q} \right), \quad (35)$$

where  $C_g/C_q$  are, respectively, the gate and quantum capacitance. The gate capacitance is given by  $C_g = \varepsilon_0 \varepsilon_r / d_0$ , where  $d_0$  is the gate separation. The quantum capacitance  $C_q$  reflects the change in the potential with the band occupancy and is defined as  $C_q = e^2 D(E)$ , where  $D(E) = g_s g_v |E| / (2 \pi \hbar^2 v_F^2)$  is the density of states. For the typical carrier densities we are interested in,  $C_g \ll C_q$ , and so the second term in Eq. (35) can be neglected. To include this effect in our model, one just needs to add  $-eU(\mathbf{r}, t)$  to the effective potential, which amounts to the substitution  $\mathcal{U}(q) \rightarrow \mathcal{U}(q) + e^2 d_0 / (\varepsilon_0 \varepsilon_r)$ . Thus, the dispersion relation becomes

$$\omega^2 = \omega_p^2 \frac{q}{k_F} + \left( S^2 + \frac{3}{4} v_F^2 \right) q^2 + \mathcal{O}(q^3), \quad (36)$$

where  $S^2 = 2e^2 v_F d_0 \sqrt{n_0} / (\hbar \varepsilon_0 \varepsilon_r \sqrt{\pi})$  is the sound velocity of the electron fluid [17]. Equation (36) is plotted in Fig. 1, alongside with Eqs. (6) and (33) for comparison. It is patent that the gate induces a linear term  $\omega \sim q$ , which rapidly dominates over the  $\sqrt{q}$  term, given a typical value for  $k_F d_0$  of the order of unit. This is a consequence of the (static) screening produced by the gate potential.

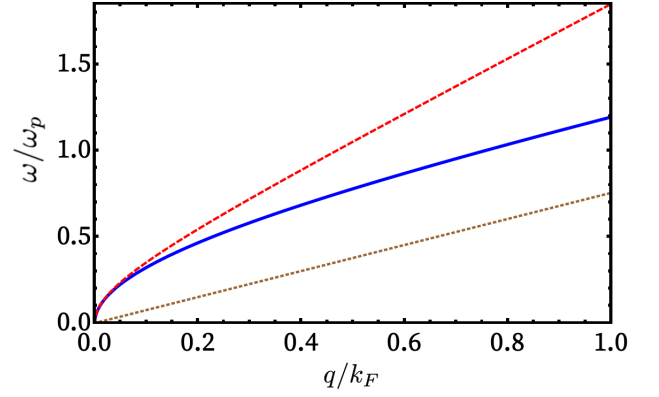


FIG. 1. Positive branch of the plasmon dispersion relation in ungated (blue) and gated (dashed red) configurations, along with the electron/hole dispersion relation  $\omega = v_F q$  (dotted brown) for  $\varepsilon_r = 2.5$  and  $d_0 k_F = 1$ . Here,  $q = |\mathbf{q}|$  is the wave vector module.

#### IV. HYDRODYNAMICAL MODEL

One of the major advantages of the present description is the possibility of calculating the moments out of Eq. (18), and subsequently construct hydrodynamical models. Since we are concerned with the diagonal elements only, we set  $W^\alpha \doteq W^{\alpha\alpha}$ . Similarly to the classical case, we define the average value of an operator  $\hat{\mathcal{G}}$  as

$$\bar{\mathcal{G}}^\alpha = \frac{1}{n^\alpha(\mathbf{r}, t)} \int d\mathbf{k} \mathcal{T}\{\hat{\mathcal{G}}\} W^\alpha(\mathbf{r}, \mathbf{k}, t), \quad (37)$$

where  $\mathbf{k} = (k_x, k_y)$  and  $\mathcal{T}\{\hat{\mathcal{G}}\}$  denotes the Weyl transform of the operator  $\hat{\mathcal{G}}$  [28],

$$\mathcal{T}\{\hat{\mathcal{G}}\} = \int \frac{d\mathbf{s}}{(2\pi\hbar)^d} e^{i\mathbf{s}\cdot\mathbf{p}/\hbar} \langle \mathbf{r} - \mathbf{s}/2 | \hat{\mathcal{G}} | \mathbf{r} + \mathbf{s}/2 \rangle, \quad (38)$$

The cases  $\hat{\mathcal{G}} = 1$  and  $\hat{\mathcal{G}} = \hat{\mathbf{k}}$  define the density and momentum variables,

$$n^\alpha(\mathbf{r}, t) = \int d\mathbf{k} W^\alpha(\mathbf{r}, \mathbf{k}, t), \quad (39)$$

$$\bar{\mathbf{p}}^\alpha(\mathbf{r}, t) = \frac{1}{n^\alpha(\mathbf{r}, t)} \int d\mathbf{k} \hbar \mathbf{k} W^\alpha(\mathbf{r}, \mathbf{k}, t). \quad (40)$$

Above, we used  $\mathcal{T}\{\hat{\mathbf{k}}\} = \mathbf{k}$  [41]. Equations (39) and (40) are valid under the assumptions that the relevant quantities are slow-varying in both space and time, which is the natural requirement to go from a microscopic field theory to a macroscopic hydrodynamical model (coarse-graining condition). The fluid description is valid if changes in the macroscopic quantities take place on small spacial and temporal scales, i.e. if  $q \ll k_F$  and  $\omega \ll \omega_p$ , respectively. This requirement is fulfilled if the characteristic time of the kinematic processes,  $t \sim 1/\omega$ , is much longer than the inverse collision frequency,  $1/\nu_c$ , and the typical length  $L$  is much greater than the mean free



path  $l \sim v_F/\nu_c$ , so that the plasma can be regarded locally as in a quasi-equilibrium configuration. However, due to the quantum nature of the model, we were able to capture the relativistic Dirac structure in a rigorous way. Actually, in the context of 2D quantum plasmas achieved in semiconductor structures, the De Broglie wavelength is replaced by the Thomas-Fermi screening length  $\lambda_{\text{TF}} = \sqrt{g_s g_v n_0} e^2 / (\sqrt{4\pi\epsilon} \hbar v_F)$ . This is the analogue of the classical Debye length in plasmas, and differs from the Fermi wavelength defined above,  $\lambda_F = 2\pi/k_F$  (ranging as  $\sim 10 \text{ nm} - 10 \mu\text{m}$  for typical graphene pa-

rameters). Consequently, the hydrodynamical limit is expected to be valid provided the condition

$$q\lambda_{\text{TF}} \ll 1, \quad q\lambda_F \ll 1. \quad (41)$$

In graphene,  $\lambda_F/\lambda_{\text{TF}} \simeq 3.2$ , such that the later condition is the most determinant of validity. Typical values of  $k_F$  are found between  $10^3$  and  $10^6 \text{ cm}^{-1}$ . At smaller wavelengths, the microscopic structure becomes important, and the hydrodynamical approximation no longer holds.

The time evolution equations for the quantities in Eqs. (39) and (40) are derived in Appendix A, and provide

$$\frac{\partial}{\partial t} n^\alpha = -\frac{2}{\hbar} \int d\mathbf{k} d\mathbf{q} i e^{i\mathbf{r} \cdot \mathbf{q}} \left[ \sinh\left(\frac{\mathbf{q}}{2} \cdot \nabla_{\mathbf{k}}\right) \xi(\mathbf{k}) \right] W^\alpha(\mathbf{q}, \mathbf{k}, t), \quad (42)$$

$$\frac{\partial}{\partial t} (n^\alpha \bar{\mathbf{p}}^\alpha) = -2 \int d\mathbf{k} d\mathbf{q} i e^{i\mathbf{r} \cdot \mathbf{q}} \mathbf{p} \left[ \sinh\left(\frac{\mathbf{q}}{2} \cdot \nabla_{\mathbf{k}}\right) \xi(\mathbf{k}) \right] W^\alpha(\mathbf{q}, \mathbf{k}, t) - \mathcal{Q}^\alpha n^\alpha \nabla \phi. \quad (43)$$

### A. Classical and semi-classical limits

In order to clarify the meaning of some of the terms in Eqs. (42) and (43), it is instructive to derive the classical limit  $\hbar \rightarrow 0$  (the semi-classical limits are obtained by keeping higher orders of  $\hbar$ ). Performing the Taylor expansion of the  $\sinh(\cdot)$  operator, we get

$$\frac{\partial}{\partial t} n^\alpha + \nabla \cdot \bar{\mathbf{j}}^\alpha = \hbar \int d\mathbf{k} \mathcal{N}\{W^\alpha\}, \quad (44)$$

$$\frac{\partial}{\partial t} (n^\alpha \bar{\mathbf{p}}^\alpha + \nabla P^\alpha + \mathcal{Q}^\alpha n^\alpha \nabla \phi) = \hbar \int d\mathbf{k} \mathbf{p} \mathcal{N}\{W^\alpha\}, \quad (45)$$

where  $\bar{\mathbf{j}}^\alpha = n^\alpha \bar{\mathbf{v}}^\alpha$  is the density current,

$$\bar{\mathbf{v}}^\alpha = \frac{v_F}{n^\alpha} \int d\mathbf{k} \frac{\mathbf{k}}{|\mathbf{k}|} W^\alpha(\mathbf{r}, \mathbf{k}, t) \quad (46)$$

is the velocity field and  $P^\alpha$  is the pressure-tensor

$$P^\alpha(\mathbf{r}, t) = v_F \int d\mathbf{k} \frac{1}{|\mathbf{p}|} \begin{pmatrix} p_x^2 & p_x p_y \\ p_y p_x & p_y^2 \end{pmatrix} W^\alpha(\mathbf{r}, \mathbf{k}, t). \quad (47)$$

The kernel  $\mathcal{N}$  introduces quantum mechanical contributions

$$\mathcal{N}\{W^\alpha\} = \sum_{n=1}^{+\infty} \frac{2\hbar^{2n-1}}{i(2n+1)!} \int d\mathbf{q} e^{i\mathbf{q} \cdot \mathbf{r}} W^\alpha(\mathbf{q}, \mathbf{k}, t) \times \left(\frac{\mathbf{q}}{2} \cdot \nabla_{\mathbf{p}}\right)^{2n+1} \xi(\mathbf{p}). \quad (48)$$

Note that, in the case of systems with parabolic dispersion,  $\xi(\mathbf{p}) = \mathbf{p}^2/(2m)$ ,  $\mathcal{N}$  vanishes. However, in the massless case, all-order derivatives of  $\xi(\mathbf{p})$  exist. By letting  $\hbar \rightarrow 0$ , we obtain the classical limit of Eqs. (44) and (45).

With the aim of obtaining semi-classical models explicitly, we consider the first-order terms of  $\mathcal{N}\{W^\alpha\}$ . Casting  $\mathcal{O}(\hbar^2)$  terms in Eq. (48), we obtain the modified hydrodynamical equations

$$\begin{aligned} \frac{\partial}{\partial t} n^\alpha + \nabla \cdot \bar{\mathbf{j}}^\alpha &= \frac{\hbar^2}{24} \left[ \frac{\partial^3}{\partial x^3} (n^\alpha \overline{J_{xxx}}^\alpha) + \frac{\partial^3}{\partial y^3} (n^\alpha \overline{J_{yyy}}^\alpha) \right. \\ &\quad \left. + 3 \frac{\partial^2}{\partial x^2} \frac{\partial}{\partial y} (n^\alpha \overline{J_{xxy}}^\alpha) + 3 \frac{\partial^2}{\partial y^2} \frac{\partial}{\partial x} (n^\alpha \overline{J_{yyx}}^\alpha) \right], \end{aligned} \quad (49)$$

$$\begin{aligned} \frac{\partial}{\partial t} (n^\alpha \bar{\mathbf{p}}^\alpha) + \nabla P^\alpha + \mathcal{Q}^\alpha n^\alpha \nabla \phi &= \frac{\hbar^2}{24} \left[ \frac{\partial^3}{\partial x^3} (n^\alpha \overline{T_{xxx}}^\alpha) \right. \\ &\quad \left. + \frac{\partial^3}{\partial y^3} (n^\alpha \overline{T_{yyy}}^\alpha) + 3 \frac{\partial^2}{\partial x^2} \frac{\partial}{\partial y} (n^\alpha \overline{T_{xxy}}^\alpha) \right. \\ &\quad \left. + 3 \frac{\partial^2}{\partial y^2} \frac{\partial}{\partial x} (n^\alpha \overline{T_{yyx}}^\alpha) \right], \end{aligned} \quad (50)$$

where  $J_{ijl}$  and  $T_{ijl}$  are the dispersive tensors

$$J_{ijl} = v_F \left( \frac{3p_i p_j p_l}{|\mathbf{p}|^5} - \frac{\delta_{ij} p_l + \delta_{jl} p_i + \delta_{li} p_j}{|\mathbf{p}|^3} \right), \quad (51)$$

$$\mathbf{T}_{ijl} = \mathbf{p} J_{ijl}. \quad (52)$$

We will provide explicit expressions for these quantities below and discuss how they modify the plasmon dispersion relation.

## B. Mass transport

Having set the relevant transport equations, we shall move now to a more detailed discussion concerning the averaged momentum and velocity fields. Once again, we are interested in the electron case, for which we shall drop the band index  $\alpha$ , for the sake of notation. As one can readily observe by comparing Eqs. (40) and (46), a proportionality relation of the form  $\bar{\mathbf{p}} = m\bar{\mathbf{v}}$  does not hold for massless particles [42]. However, by allowing a space and time dependence on the mass, we are able to define an effective “mass tensor” as

$$m_{ij}(\mathbf{r}, t) = \frac{\bar{p}_i(\mathbf{r}, t)}{\bar{v}_i(\mathbf{r}, t)} \delta_{ij},$$

$$= \frac{\hbar}{v_F} \frac{\int d\mathbf{k} \, k_i W(\mathbf{r}, \mathbf{k}, t)}{\int d\mathbf{k} \, k_i W(\mathbf{r}, \mathbf{k}, t)/|\mathbf{k}|} \delta_{ij}, \quad (53)$$

and the corresponding “mass density tensor”  $\rho_{ij} = nm_{ij}$ . The meaning of such fields should be clear: although the carriers have no mass (Dirac particles), the fluid velocity and momentum fields can be related via an effective mass, providing a measure of the inertia of a fluid element. Due to rotational symmetry, we must have  $m_{ij}(\mathbf{r}, t) = m(\mathbf{r}, t)\delta_{ij}$ .

We now modify the equilibrium used in the last section in order to describe adiabatic (hydrodynamic) changes in the system,

$$W(\mathbf{r}, \mathbf{k}, t) = \frac{n_0}{\pi k_F^2} \Theta \left( k_F - n_0 \left| \frac{\mathbf{k} - \bar{\mathbf{k}}(\mathbf{r}, t)}{n(\mathbf{r}, t)} \right| \right). \quad (54)$$

This particular form of the equilibrium is consistent with the definitions (39) and (40). Without loss of generality, we can assume  $\bar{k}_y = 0$ . Plugging Eq. (54) into the  $x$ -component of Eq. (46), it leads to

$$\bar{v}_x(\mathbf{r}, t) = \frac{\bar{p}_x(\mathbf{r}, t)}{\mathcal{M}\gamma(\mathbf{r}, t)}, \quad (55)$$

where  $\mathcal{M} = \hbar k_F/v_F$  is the Drude mass and  $\gamma$  is the Lorentz-like factor,

$$\gamma^{-1}(n, \bar{p}_x) = \frac{8}{\pi} \int_0^1 dy \frac{\sqrt{1-y^2}}{\sqrt{f_+} + \sqrt{f_-}}, \quad (56)$$

$$f_{\pm} = \left( p' \pm n' \sqrt{1-y^2} \right)^2 + y^2, \quad p' = \frac{\bar{p}_x}{p_F}, \quad n' = \frac{n}{n_0}.$$

As we can see,  $\gamma$  depends on the position and time merely through the hydrodynamical variables  $n(\mathbf{r}, t)$  and  $\bar{p}_x(\mathbf{r}, t) = \hbar \bar{k}_x(\mathbf{r}, t)$ .

Although the integral in Eq. (56) has no analytic solution in general, it admits amenable forms in the limiting cases of small and large momenta. We can verify that  $(\partial\gamma/\partial\bar{p}_x)|_{\bar{p}_x=0} = 0$ , thus for  $\bar{p}_x/p_F \ll 1$ ,  $\gamma$  becomes

$$\gamma(n) \simeq \frac{\pi}{4} \frac{1 - n^2/n_0^2}{K_1(1 - n^2/n_0^2) - K_2(1 - n^2/n_0^2)}, \quad (57)$$

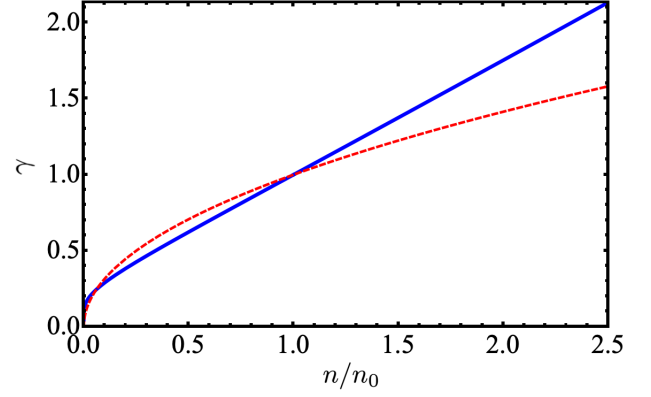


FIG. 2. Graphical representation of Eq. (57) (solid blue), as a function of the normalised density  $n' = n/n_0$ , evaluated in the limit  $\bar{p}_x/p_F \ll 1$ , which verifies  $\gamma(n') \sim \pi n'/4$  for  $n' \gg 1$ ;  $\gamma(n') = \sqrt{n'}$  (dashed red), which has been adopted in the literature.

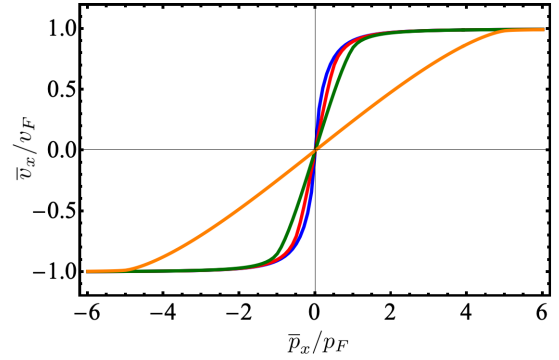


FIG. 3. Exact relation between average velocity and momentum fields, for several values of the normalised density  $n' = n/n_0$ . Near the origin, we find a linear relation between both variables, while for large momentum, the velocity converges, in absolute value, to the Fermi velocity, becoming only a function of the sign of  $\bar{p}_x$ .

where  $K_1(x) = \int_0^{\pi/2} d\theta (1 - x^2 \sin^2 \theta)^{-1/2}$  and  $K_2(x) = \int_0^{\pi/2} d\theta (1 - x^2 \sin^2 \theta)^{1/2}$  are the complete elliptic integrals of the first and second kind, respectively. Accordingly, the quantities  $\bar{p}_x$  and  $\bar{v}_x$  become proportional to each other, ensuring a relation of the form  $\bar{p}_x = m(n)\bar{v}_x$ . In the case  $n = n_0$ ,  $m = \mathcal{M}$ , as  $\gamma(n_0) = 1$ . For general out-of-equilibrium conditions with small values of  $\bar{p}_x/p_F$ , the mass differs from the Drude mass, as  $m(n) = \gamma(n)\mathcal{M}$ , with  $\gamma(n)$  depicted in Fig. 2. We also plot the commonly adopted expression  $\gamma(n) = \sqrt{n/n_0}$ , for comparison. This form of  $\gamma$  leads to the effective mass  $m = \mathcal{M}\sqrt{n'}$ , which is based on the local approximation for the Fermi wavevector,  $k_F = \sqrt{\pi n_0} \rightarrow \sqrt{\pi n(\mathbf{r}, t)}$  [1, 42, 43]. Equation (57) results in significant changes, when compared to the latter, with a functional dependence on  $n$  which strongly differs from proposed  $\sqrt{n}$  behaviour, specially in the case of  $n' \gg 1$  (see Fig. 2).

For  $\bar{p}_x/p_F \gg 1$ , we find  $\gamma \simeq |\bar{p}_x|/(v_F \mathcal{M})$ . This implies  $\bar{v}_x \simeq \text{sign}(\bar{p}_x)v_F$ , meaning that, for large fluid momentum, the fluid velocity approaches the Fermi velocity. In Fig. 3, we can observe that a linear relation between momentum and velocity holds for small velocities only.

### C. Semi-classical dispersion relation

Next, we provide analytical expressions for the quantities appearing in Eqs. (47), (51) and (52) - in terms of the previous hydrodynamical variables  $n^\alpha$  and  $\bar{\mathbf{p}}^\alpha$  - via Eq. (54). We restrict, yet again, the variations to the  $x$ -direction, such that the relevant quantities are  $\bar{J}_{xx}$ ,  $\bar{T}_{xxx}$  and  $P_{xx}$ . Considering

$$n(x, t) \simeq n_0 + \tilde{n}(x, t), \quad \bar{p}_x(x, t) \simeq \bar{p}_{x,0} + \tilde{\bar{p}}_x(x, t). \quad (58)$$

and neglecting second order terms, the relevant components featuring the hydrodynamical equations read (see Appendix B)

$$P_{xx} \simeq p_F v_F n_0 \left( \frac{1}{3} + \frac{3}{4} \frac{\tilde{n}}{n_0} \right), \quad (59)$$

$$\bar{J}_{xxx} \simeq -\frac{3v_F}{4p_F^3} \tilde{\bar{p}}_x, \quad (60)$$

$$\bar{T}_{xxx} \simeq \frac{3v_F}{p_F} \left( \frac{1}{4} - \frac{1}{8} \frac{\tilde{n}}{n_0} \right), \quad (61)$$

Keeping only the  $\mathcal{O}(\tilde{n})$  terms in Eq. (57), we find

$$\gamma(\tilde{n}) \simeq 1 + \frac{3}{4} \frac{\tilde{n}}{n_0}, \quad (62)$$

which leads to linearized velocity

$$\bar{v}_x \simeq \frac{\tilde{\bar{p}}_x}{\mathcal{M}}. \quad (63)$$

By combining the latter results, we obtain

$$\frac{\partial}{\partial t} \tilde{n} + \frac{\partial}{\partial x} \left( n_0 \frac{\tilde{\bar{p}}_x}{\mathcal{M}} \right) = -\frac{\hbar^2}{24} \frac{\partial^3}{\partial x^3} \left( n_0 \frac{3v_F}{4p_F^3} \tilde{\bar{p}}_x \right), \quad (64)$$

$$\frac{\partial}{\partial t} (n_0 \tilde{\bar{p}}_x) + \frac{\partial}{\partial x} \left( \frac{3}{4} p_F v_F \tilde{n} \right) + \mathcal{Q} n_0 \frac{\partial}{\partial x} \tilde{\phi} = \frac{\hbar^2}{24} \frac{\partial^3}{\partial x^3} \left( \frac{3v_F}{8p_F} \tilde{n} \right), \quad (65)$$

where  $\tilde{\phi}(\mathbf{r}, t)$  is the perturbed electrostatic potential,

$$\tilde{\phi}(\mathbf{r}, t) = \frac{\mathcal{Q}}{4\pi\epsilon_0\epsilon_r} \int d\mathbf{r}' \frac{\tilde{n}(x, t)}{|\mathbf{r} - \mathbf{r}'|}, \quad (66)$$

and  $\mathcal{Q} = e$ . Fourier analysis of Eqs. (64) and (65) leads to the modified plasmon dispersion

$$\omega^2 = \omega_p^2 \frac{q}{k_F} + \frac{3}{4} v_F^2 q^2 - \frac{\omega_p^2}{32} \frac{q^3}{k_F^3} + \nu \frac{\hbar^2 q^4}{4\mathcal{M}^2}, \quad (67)$$

where  $\nu = -1/32$  is a numerical factor resulting from the contributions of both  $\bar{J}_{xxx}$  and  $\bar{T}_{xxx}$ . The two first terms

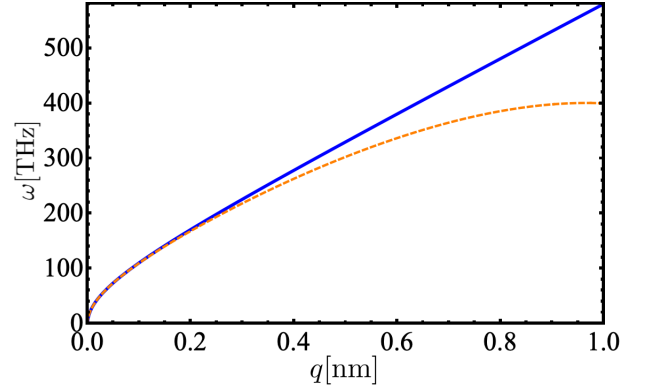


FIG. 4. Positive branch of the semi-classical plasmon dispersion relation in Eq. (67) (orange dashed), together with its classical counterpart, given by Eq. (33) (blue), with  $\epsilon_r = 2.5$ .

in the r.h.s are in agreement with Eq. (33), and the third term is a classical ( $\hbar$ -independent) contribution to the plasmon dispersion. The fourth one accounts for a quantum correction ( $\sim \hbar^2$ ), and is a consequence of the Bohm potential [44], which plays the role of a quantum pressure. For Dirac plasmas, we find a negative sign in the quantum correction (the Bohm pressure softens the plasmon mode), contrary to the what has been reported for the case of parabolic particles,  $\hbar^2 q^4/(4m^2)$  [45, 46]. Since the absolute value of  $\nu$  is rather small, such correction only becomes important for intermediate wave-number values, as can be seen in Fig. 4. The plasmon dispersion relation of Eq. (67) indicates that the present quantum hydrodynamical model is superior to the RPA calculation performed in previous chapters, as the latter hides the effect of Bohm dispersion, which is known to play an important role in the case of dense plasmas. [45, 47].

## V. CONCLUSIONS AND FUTURE WORK

Using the Wigner-Moyal description, we have derived a quantum hydrodynamical model for a Dirac electron-hole plasma in single-layer graphene. The massless nature of the quasi-particles was captured by the low-energy limit of the many-body Hamiltonian, which served as the basis for the construction of the Wigner matrix. Then, the equation of motion for the Wigner matrix elements in the phase-space was established, with the interacting potential being given by the Hartree approximation. The latter turns out to be an excellent approximation for graphene, as the coupling constant is very small,  $r_s \sim \alpha_s/\epsilon_r \ll 1$ , and independent of the electron density. Moreover, a closed set of generalised quantum hydrodynamical equations was derived by taking the moments of the quantum kinetic equation. We found an infinite number of  $\hbar$ -dependent terms arising in both the continuity and force equations, as a consequence of the linear dispersion relation of the carriers. As it is shown, in the con-



ventional case of parabolic systems (i.e. for which the single-particle dispersion relation is  $\sim p^2$ ), these contributions vanish. To the best of our knowledge, such corrections have not been discussed so far in the literature. By neglecting the quantum corrections, our model reduces to existing semi-classical models for Dirac fermions [18, 20, 43]. Moreover, a nonlinear relation between the fluid velocity and momentum fields have been put forward in order to construct a hydrodynamical mass. We found a relation of the form  $\bar{\mathbf{p}} = \gamma(\mathbf{r}, t)\mathcal{M}\bar{\mathbf{v}}$ , where  $\mathcal{M}$  is the Drude mass and  $\gamma(\mathbf{r}, t)$  is a local Lorentz-like factor. In the limiting cases of small and large averaged momentum,  $\gamma(\mathbf{r}, t)$  is given analytically. Up to first order in both the density and momentum fluctuations, we find  $\bar{\mathbf{p}} \simeq \mathcal{M}\bar{\mathbf{v}}$ . We stress the fact that a quantitative description for the hydrodynamical mass is a major issue in the current research, therefore being one important result of the current kinetic description. We have also computed higher-order corrections to the plasmon dispersion relation ( $\sim q^4$ ) by taking into account the first quantum corrections to the hydrodynamical equations.

We expect our formalism to be particularly suited to describe out-of-equilibrium quantum dynamics of Dirac electrons in a more systematic manner. While the linear response can be indeed described within the framework RPA (which we recover upon linearization of the Wigner equation), the nonlinear regimes deserve a more complete description, which are captured by the kinetic equation that we have proposed here. This is crucial in the description of saturation in the late stages of dynamical instabilities, for example. Moreover, (quantum) diffusive

processes may be captured by adapting the strategy of quasi-linear theories accounting for particle-wave interactions [48]; by working out the collision integral at different levels of approximation, we may obtain quantum versions of the Fokker-Planck equation for relativistic-like particles. Another interesting aspect of our work is the contribution to the hydrodynamical modelling of graphene plasmas. With the ab-initio establishment of a hydrodynamical mass, we are able to simulate experimentally relevant configurations, such as hydrodynamical instabilities in field-effect transistor THz emitters [17]. Moreover, at a phenomenological level, our hydrodynamical model is particularly suited to accommodate both shear and odd (or Hall) viscosity terms (while a more microscopic, kinetic theory is more demanding, involving the details of the processes leading to dissipation). The latter has been identified to play a special role in the topology of acoustic waves [49], and we hope that plasmons may also feature such topological transitions, opening the venue for a range of applications.

## ACKNOWLEDGMENTS

H. T. acknowledges Fundação para a Ciência e Tecnologia (FCT-Portugal) through the Contract No. CEECIND/00401/2018 and J. P. B. acknowledges the financial support from the Quantum Flagship Grant PhoQuS (Grant No. 820392) of the European Union.

## A. DERIVATION OF THE HYDRODYNAMICAL SET OF EQUATIONS

In this section, we derive the hydrodynamical set of Eqs. (42) and (43). To do that, we start by time differentiating Eqs. (39) and (40) (timed  $n^\alpha$ ), and replace  $\partial_t W^\alpha(\mathbf{r}, \mathbf{k}, t)$  by  $\int d\mathbf{q} e^{i\mathbf{q}\cdot\mathbf{r}} \partial_t W^\alpha(\mathbf{q}, \mathbf{k}, t)$ , given that Eq. (18) only provides time derivatives of the Wigner matrix components in Fourier space. We get

$$\frac{\partial}{\partial t} n^\alpha = -\frac{1}{\hbar} \int d\mathbf{k} d\mathbf{q} i e^{i\mathbf{r}\cdot\mathbf{q}} \Delta\xi^-(\mathbf{q}, \mathbf{k}) W^\alpha(\mathbf{q}, \mathbf{k}, t) - e \int d\mathbf{q} d\mathbf{q}' i e^{i\mathbf{q}\cdot\mathbf{r}} \phi(\mathbf{q}', t) \int d\mathbf{k} \Delta W^{\alpha\alpha}(\mathbf{q}, \mathbf{k}, \mathbf{q}', t), \quad (68)$$

$$\frac{\partial}{\partial t} (n^\alpha \bar{\mathbf{p}}^\alpha) = - \int d\mathbf{k} d\mathbf{q} i e^{i\mathbf{r}\cdot\mathbf{q}} \mathbf{k} \Delta\xi^-(\mathbf{q}, \mathbf{k}) W^\alpha(\mathbf{q}, \mathbf{k}, t) - e \int d\mathbf{q} d\mathbf{q}' i e^{i\mathbf{q}\cdot\mathbf{r}} \phi(\mathbf{q}', t) \int d\mathbf{k} \mathbf{k} \Delta W^{\alpha\alpha}(\mathbf{q}, \mathbf{k}, \mathbf{q}', t), \quad (69)$$

where  $n^\alpha \doteq n^\alpha(\mathbf{r}, t)$  and  $\bar{\mathbf{p}}^\alpha \doteq \bar{\mathbf{p}}^\alpha(\mathbf{r}, t)$ . Now, we use the following relations

$$\Delta W^{\alpha\alpha}(\mathbf{q}, \mathbf{k}, \mathbf{q}', t) = -2s^\alpha e^{-\mathbf{q}'\cdot\nabla_{\mathbf{q}}} \sinh\left(\frac{\mathbf{q}'}{2} \cdot \nabla_{\mathbf{k}}\right) W^\alpha(\mathbf{q}, \mathbf{k}, t), \quad (70)$$

$$\Delta\xi^-(\mathbf{q}, \mathbf{k}) = 2 \sinh\left(\frac{\mathbf{q}}{2} \cdot \nabla_{\mathbf{k}}\right) \xi(\mathbf{k}), \quad (71)$$

into Eqs. (68) and (69), which leads to

$$\begin{aligned} \frac{\partial}{\partial t} n^\alpha = & -\frac{2}{\hbar} \int d\mathbf{k} d\mathbf{q} i e^{i\mathbf{r}\cdot\mathbf{q}} \left[ \sinh\left(\frac{\mathbf{q}}{2} \cdot \nabla_{\mathbf{k}}\right) \xi(\mathbf{k}) \right] W^\alpha(\mathbf{q}, \mathbf{k}, t) \\ & + 2\mathcal{Q}^\alpha \int d\mathbf{q} d\mathbf{q}' i e^{i\mathbf{q}\cdot\mathbf{r}} \phi(\mathbf{q}', t) e^{-\mathbf{q}'\cdot\nabla_{\mathbf{q}}} \int d\mathbf{k} \sinh\left(\frac{\mathbf{q}'}{2} \cdot \nabla_{\mathbf{k}}\right) W^\alpha(\mathbf{q}, \mathbf{k}, t), \end{aligned} \quad (72)$$

$$\begin{aligned} \frac{\partial}{\partial t} (n^\alpha \bar{\mathbf{p}}^\alpha) = & -2 \int d\mathbf{k} d\mathbf{q} i e^{i\mathbf{r}\cdot\mathbf{q}} \mathbf{k} \left[ \sinh\left(\frac{\mathbf{q}}{2} \cdot \nabla_{\mathbf{k}}\right) \xi(\mathbf{k}) \right] W^\alpha(\mathbf{q}, \mathbf{k}, t) \\ & + 2\mathcal{Q}^\alpha \int d\mathbf{q} d\mathbf{q}' i e^{i\mathbf{q}\cdot\mathbf{r}} \phi(\mathbf{q}', t) e^{-\mathbf{q}'\cdot\nabla_{\mathbf{q}}} \int d\mathbf{k} \mathbf{k} \sinh\left(\frac{\mathbf{q}'}{2} \cdot \nabla_{\mathbf{k}}\right) W^\alpha(\mathbf{q}, \mathbf{k}, t). \end{aligned} \quad (73)$$

In 2D, the differential operator  $\sinh\left(\frac{\mathbf{q}'}{2} \cdot \nabla_{\mathbf{k}}\right)$  reads

$$\sinh\left(\frac{\mathbf{q}'}{2} \cdot \nabla_{\mathbf{k}}\right) = \sum_{n=0}^{+\infty} \sum_{m=0}^{2n+1} \theta_{nm} \left(\frac{q'_x}{2} \frac{\partial}{\partial k_x}\right)^m \left(\frac{q'_y}{2} \frac{\partial}{\partial k_y}\right)^{2n+1-m} = \frac{\mathbf{q}'}{2} \cdot \nabla_{\mathbf{k}} + \mathcal{O}\left(\frac{\partial^3}{\partial k_i^3}\right), \quad (74)$$

where  $\theta_{nm} = 1/[m!(2n+1-m)!]$ . By plugging Eq. (74) into the second term on the r.h.s. of Eq. (72), we get a sum of terms, all of them at least linear in the derivatives in  $\mathbf{k}$ . Once the remaining integrand is  $\mathbf{k}$ -independent, we can perform partial integration in  $\mathbf{k}$ , which reduces to surface contributions. Assuming that the Wigner matrix elements and all order  $\mathbf{k}$ -derivatives go to zero as  $k_i \rightarrow \pm\infty$ , we readily obtain Eq. (42). By repeating the same procedure, a similar argument allows to simplify the last term on the r.h.s. of Eq. (73). However, in this case, the remaining integrand is linear in  $\mathbf{k}$ , which gives a non-trivial contribution, coming from the first term of Eq. (74). Therefore, we obtain

$$\begin{aligned} \frac{\partial}{\partial t} (n^\alpha \bar{\mathbf{p}}^\alpha) = & -2 \int d\mathbf{k} d\mathbf{q} i e^{i\mathbf{r}\cdot\mathbf{q}} \mathbf{k} \left[ \sinh\left(\frac{\mathbf{q}}{2} \cdot \nabla_{\mathbf{k}}\right) \xi(\mathbf{k}) \right] W^\alpha(\mathbf{q}, \mathbf{k}, t) \\ & - \mathcal{Q}^\alpha \int d\mathbf{q} d\mathbf{q}' d\mathbf{r}' i e^{i\mathbf{q}\cdot\mathbf{r}} \mathbf{q}' \phi(\mathbf{q}', t) e^{-\mathbf{q}'\cdot\nabla_{\mathbf{q}}} \frac{e^{-i\mathbf{q}\cdot\mathbf{r}'}}{(2\pi)^2} \cdot n^\alpha(\mathbf{r}', t). \end{aligned} \quad (75)$$

Above, we used the property  $\int d\mathbf{k} W^\alpha(\mathbf{q}, \mathbf{k}, t) = n^\alpha(\mathbf{q}, t)$ , which follows from Fourier transforming Eq. (15), and further replaced  $n^\alpha(\mathbf{q}, t)$  by  $\int d\mathbf{r}' e^{-i\mathbf{q}'\cdot\mathbf{r}'} n^\alpha(\mathbf{r}', t) (2\pi)^{-2}$ . Using the identities  $e^{-\mathbf{q}'\cdot\nabla_{\mathbf{q}}} e^{-i\mathbf{q}\cdot\mathbf{r}'} = e^{i(\mathbf{q}'-\mathbf{q})\cdot\mathbf{r}'}$ ,  $i\mathbf{q} e^{i\mathbf{q}\cdot\mathbf{r}} = \nabla e^{i\mathbf{q}\cdot\mathbf{r}}$  and  $\int d\mathbf{q} e^{i(\mathbf{r}-\mathbf{r}')\cdot\mathbf{q}} (2\pi)^{-2} = \delta(\mathbf{r}-\mathbf{r}')$ , we finally arrive at Eq. (43).

## B. CALCULATION OF THE DISPERSIVE TENSORS

Plugging Eq. (54) into the relevant components of Eqs. (47), (51) and (52) gives

$$P_{xx} = \frac{\hbar v_F n_0}{\pi k_F^2} \int_0^{k_F} dk_y \left[ k_+(k_+^2 + k_y^2)^{1/2} - k_-(k_-^2 + k_y^2)^{1/2} - k_y^2 \log\left(\frac{k_+(k_-^2 + k_y^2)^{1/2}}{k_-(k_+^2 + k_y^2)^{1/2}}\right) \right]. \quad (76)$$

$$\overline{J_{xxx}} = \frac{2v_F n_0}{\pi p_F^2 n} \int_0^{k_F} dk_y k_y^2 \left[ \frac{1}{(k_+^2 + k_y^2)^{1/2}} - \frac{1}{(k_-^2 + k_y^2)^{1/2}} \right], \quad (77)$$

$$\overline{T_{xxx}^x} = \frac{2\hbar v_F n_0}{\pi p_F^2 n} \int_0^{k_F} dk_y \left[ \frac{k_-^3}{(k_-^2 + k_y^2)^{3/2}} - \frac{k_+^3}{(k_+^2 + k_y^2)^{1/2}} \right], \quad (78)$$

where  $k_{\pm} = \bar{k}_x \pm n' \sqrt{k_F^2 - k_y^2}$  and  $n' = n/n_0$ . For the equilibrium configuration, we expect to have  $\bar{p}_{x,0} = 0$ , such that only the first order term contributes. Expanding Eqs. (76)–(78) and neglecting  $\mathcal{O}(\tilde{p}_x^2/p_F^2)$  terms, it leads to

$$\overline{J_{xxx}} \simeq \frac{4v_F}{\pi p_F^3} \frac{n_0/n}{(n^2/n_0^2 - 1)^2} \left[ 2K_1 \left( 1 - \frac{n_0^2}{n^2} \right) - \left( 1 + \frac{n^2}{n_0^2} \right) K_2 \left( 1 - \frac{n_0^2}{n^2} \right) \right] \tilde{p}_x, \quad (79)$$

$$\overline{T_{xxx}} \simeq \frac{4v_F}{\pi p_F} \frac{n/n_0}{(n^2/n_0^2 - 1)^2} \left[ 2K_1 \left( 1 - \frac{n_0^2}{n^2} \right) - \left( 1 + \frac{n^2}{n_0^2} \right) K_2 \left( 1 - \frac{n_0^2}{n^2} \right) \right], \quad (80)$$

$$P_{xx} \simeq \frac{4p_F v_F n_0}{3\pi} \frac{1}{n^2/n_0^2 - 1} \left[ \frac{n^4}{n_0^4} K_2 \left( 1 - \frac{n_0^2}{n^2} \right) - \frac{n^2}{n_0^2} K_1 \left( 1 - \frac{n_0^2}{n^2} \right) \right]. \quad (81)$$

Keeping only the  $\mathcal{O}(n)$  terms in Eqs. (79)–(81), it yields Eqs. (59)–(61).

- 
- [1] A. H. Castro Neto, F. Guinea, N. M. R. Peres, K. S. Novoselov, and A. K. Geim, *Rev. Mod. Phys.* **81**, 109 (2009).
  - [2] E. H. Hwang and S. Das Sarma, *Phys. Rev. B* **75**, 205418 (2007).
  - [3] P. R. Wallace, *Phys. Rev.* **71**, 622 (1947).
  - [4] D. Rodrigo, O. Limaj, D. Janner, D. Etezadi, F. J. Garcia de Abajo, V. Pruneri, and H. Altug, *Science* **349**, 165–168 (2015).
  - [5] J. Chen, M. Badioli, P. Alonso-González, S. Thongratanasiri, F. Huth, J. Osmond, M. Spasenović, A. Centeno, A. Pesquera, P. Godignon, and et al., *Nature* **487**, 77–81 (2012).
  - [6] S. Zeng, K. V. Sreekanth, J. Shang, T. Yu, C.-K. Chen, F. Yin, D. Baillargeat, P. Coquet, H.-P. Ho, A. V. Kabashin, and K.-T. Yong, *Advanced Materials* **27**, 6163 (2015).
  - [7] F. H. L. Koppens, D. E. Chang, and F. J. García de Abajo, *Nano Letters* **11**, 3370 (2011), pMID: 21766812.
  - [8] A. Agarwal, M. Vitiello, L. Viti, A. Cupo-lillo, and A. Politano, *Nanoscale* **10** (2018), 10.1039/C8NR01395K.
  - [9] S. Dai, Z. Fei, Q. Ma, A. S. Rodin, M. Wagner, A. S. McLeod, M. K. Liu, W. Gannett, W. Regan, K. Watanabe, T. Taniguchi, M. Thiemens, G. Dominguez, A. H. C. Neto, A. Zettl, F. Keilmann, P. Jarillo-Herrero, M. M. Fogler, and D. N. Basov, *Science* **343**, 1125 (2014).
  - [10] Y. Lin, T. V. Williams, and J. W. Connell, *The Journal of Physical Chemistry Letters* **1**, 277 (2009).
  - [11] Y. Li, Z. Li, C. Chi, H. Shan, L. Zheng, and Z. Fang, *Advanced Science* **4**, 1600430 (2017).
  - [12] A. N. Grigorenko, M. Polini, and K. S. Novoselov, *Nature Photonics* **6**, 749 (2012).
  - [13] A. Geim and K. Novoselov, *Nature materials* **6**, 183 (2007).
  - [14] Y. Yang, Z. Shi, J. Li, and Z.-Y. Li, *Photonics Research* **4**, 65 (2016).
  - [15] F. Wang, Y. Zhang, C. Tian, C. Girit, A. Zettl, M. Crommie, and Y. R. Shen, *Science* **320**, 206 (2008).
  - [16] L. B. N. Laboratory, U. S. D. of Energy. Office of Scientific, and T. Information, *Dirac Charge Dynamics in Graphene by Infrared Spectroscopy* (Lawrence Berkeley National Laboratory, 2008).
  - [17] P. Cosme and H. Terças, *ACS Photonics* **7**, 1375 (2020).
  - [18] V. Ryzhii, A. Satou, and T. Otsuji, *Journal of Applied Physics - J APPL PHYS* **101** (2007), 10.1063/1.2426904.
  - [19] R. Bistritzer and A. H. MacDonald, *Phys. Rev. B* **80**, 085109 (2009).
  - [20] D. Svintsov, V. Vyurkov, S. Yurchenko, T. Otsuji, and V. Ryzhii, *Journal of Applied Physics* **111**, 083715 (2012).
  - [21] U. Schwengelbeck, L. Plaja, L. Roso, and E. C. Jarque, *Journal of Physics B: Atomic, Molecular and Optical Physics* **33**, 1653 (2000).
  - [22] R. Jasiak, G. Manfredi, P.-A. Hervieux, and M. Haefele, *New Journal of Physics* **11**, 063042 (2009).
  - [23] T. V. Teperik, P. Nordlander, J. Aizpurua, and A. G. Borisov, *Phys. Rev. Lett.* **110**, 263901 (2013).
  - [24] V. K. Dugaev and M. I. Katsnelson, *Phys. Rev. B* **88**, 235432 (2013).
  - [25] E. Wigner, *Phys. Rev.* **40**, 749 (1932).
  - [26] G. Catarina, B. Amorim, E. V. Castro, J. M. V. P. Lopes, J. M. V. P. Lopes, and N. Peres, “Twisted bilayer graphene: Low-energy physics, electronic and optical properties,” in *Handbook of Graphene Set* (John Wiley & Sons, Ltd, 2019) Chap. 6, pp. 177–231.
  - [27] J. E. Moyal, *Proc. Cambridge Phil. Soc.* **45**, 99 (1949).
  - [28] H. Weyl, *Z. Phys.* **46** (2002).
  - [29] M. Hillery, R. F. O’Connell, M. O. Scully, and E. P. Wigner, “Distribution functions in physics: Fundamentals,” in *Part I: Physical Chemistry. Part II: Solid State Physics* (Springer Berlin Heidelberg, Berlin, Heidelberg, 1997) pp. 273–317.
  - [30] T. Stauber, N. M. R. Peres, and F. Guinea, *Phys. Rev. B* **76**, 205423 (2007).
  - [31] A. L. Fetter and J. D. Walecka, *Quantum Theory of Many-Particle Systems* (McGraw-Hill, Boston, 1971).
  - [32] S. Das Sarma and E. H. Hwang, *Physical Review Letters* **102** (2009), 10.1103/physrevlett.102.206412.
  - [33] B. Wunsch, T. Stauber, F. Sols, and F. Guinea, *New Journal of Physics* **8**, 318 (2006).
  - [34] S. Das Sarma, E. Hwang, and Q. Li, *Phys. Rev. B* **80** (2009), 10.1103/PhysRevB.80.121303.
  - [35] S. Adam, E. H. Hwang, V. M. Galitski, and S. Das Sarma, *Proceedings of the National Academy of Sciences* **104**, 18392–18397 (2007).
  - [36] C. Kittel, *Quantum Theory of Solids* (John Wiley and Sons, Inc, 1963).

- [37] B. Eliasson and C. S. Liu, *Physics of Plasmas* **25**, 012105 (2018).
- [38] B. Wunsch, T. Stauber, F. Sols, and F. Guinea, *New Journal of Physics* **8**, 318 (2006).
- [39] Y. Liu, R. Willis, K. Emtsev, and T. Seyller, *Phys. Rev. B* **78** (2008), 10.1103/PhysRevB.78.201403.
- [40] W. Zhu, V. Perebeinos, M. Freitag, and P. Avouris, *Phys. Rev. B* **80**, 235402 (2009).
- [41] *This can be proved directly from the definition in (38), after performing the coordinate transformation  $\mathbf{s} = \mathbf{r} - \mathbf{z}/2$ , together with the relation  $\langle \mathbf{r} | \hat{\mathbf{k}} | \mathbf{r}' \rangle = -i \nabla \delta(\mathbf{r} - \mathbf{r}')$ .*
- [42] A. J. Chaves, N. M. R. Peres, G. Smirnov, and N. A. Mortensen, *Physical Review B* **96** (2017), 10.1103/physrevb.96.195438.
- [43] D. Svintsov, V. Vyurkov, V. Ryzhii, and T. Otsuji, *Physical Review B* **88** (2013), 10.1103/physrevb.88.245444.
- [44] M.-J. Lee and Y.-D. Jung, *Physics Letters A* **381**, 636 (2017).
- [45] M. Akbari-Moghanjoughi, *Physics of Plasmas* **19**, 042701 (2012), <https://doi.org/10.1063/1.3699535>.
- [46] G. Manfredi and F. Haas, *Phys. Rev. B* **64**, 075316 (2001).
- [47] S.-C. Li, *Physics of Plasmas* **17**, 082307 (2010).
- [48] D. Nicholson, *Introduction to Plasma Theory* (Wiley, 1983).
- [49] A. Souslov, K. Dasbiswas, M. Fruchart, S. Vaikuntanathan, and V. Vitelli, *Phys. Rev. Lett.* **122**, 128001 (2019).